Chem. Mater. **1999,** *11,* 3015−3017

Self-Organization of Ordered Silver Nanocrystal Arrays on Cubic Mesoporous Silica Surfaces

Lian-Zhou Wang, Jian-Lin Shi,* Wen-Hua Zhang, Mei-Ling Ruan, Jian Yu, and Dong-Sheng Yan

The State Key Lab of High Performance Ceramics and Superfine Microstructure, Shanghai Institute of Ceramics, Chinese Academy of Science, Shanghai 200050, China

Received April 19, 1999
Revised Manuscript Received August 26, 1999

The self-assembly of nanoparticles into ordered morphologies is one of the topics in focus in the field of materials science as it is expected to create nanostructured materials with unique physical and chemical properties.[1−4] To prepare these novel materials, some techniques have been developed in organizing the nanocrystalline metal, metal oxide, or semiconductor into ordered aggregates or superlattices.[5−11] The ability to assemble nanoparticles into well-defined configurations provides opportunities for exploring undocumented properties of materials and offer possibilities for potential applications.

Mesoporous silica materials possessing well-ordered and controllable mesopores with a narrow pore size distribution have stimulated great interest, owing to their potential applications in catalysis, adsorption, nanotechnology, etc.[12−15] The periodic mesoporous materials, mainly ordered hexagonal MCM-41 and cubic MCM-48, provide perfect candidates for the loading and encapsulation of metal or semiconductor clusters and nanowires.[16,17] In this communication, regular and oriented silver nanocrystal line arrays loaded on the surface of cubic mesoporous silica MCM-48 material are obtained for the first time by an approach of impregnation followed by thermal treatment.

The cubic MCM-48 material was synthesized as follows: an aqueous solution of surfactant cetyltrimethylammonium bromide C_{16}TMABr, a sodium hydroxide solution, and tetraethyl orthosilicate were well mixed to obtain a gel with a molar composition of 0.48C_{16}TMABr:1TEOS:0.6NaOH:65H_2O. After the gels were stirred for 3 h, they were loaded in PTFE-lined stainless steel autoclaves and heated at 110 °C for 24 h, and then the precipitated products were filtered, washed with distilled water, and heated in a drying oven at 60 °C. The as-synthesized sample was calcined in air at 540 °C for 6 h to remove the surfactants, designated as sample PS (pure silica). An impregnating method via the route of vacuum filling was employed as the procedure for Ag-loaded MCM-48 material. A total of 0.5 g of MCM-48 material was degassed at 150 °C in a vacuum for 8 h and then cooled to room temperature. Three milliliters of 0.1 M $AgNO_3$ ethanol solution was dropped onto the sample under vacuum until the sample was fully soaked by the solution. Afterward, the sample was allowed to dry at room temperature (named as AS), and then part of the sample AS was given a thermal treatment at 300 °C for 2 h (designated as AST). The X-ray powder diffraction measurements of samples were recorded on a Rigaku D/Max-Π X-ray diffractometer with Cu Kα radiation. Pore structures of materials were observed with a JEOL-200 CX electron microscope operated at 200 keV. N_2 adsorption−desorption isotherms were measured at 77 K using a Micromeritics ASAP 2400 analyzer. The specific surface area (S_{BET}) of samples was determined from the linear part of BET plot ($P/P_0 = 0.05-0.15$). The pore size distribution (PSD) of samples was calculated using the Barrett−Joyner−Halenda (BJH) formula.

The X-ray diffraction patterns of the samples are shown in Figure 1. The peaks at low 2θ range (2−10°) shows clearly the characteristics of cubic MCM-48 materials for each sample. XRD pattern of sample AS (Figure 1a) shows no strong peak of Ag or its compound at the high 2θ range (10−80°). However, upon thermal treatment, the color of sample AST turns from white to black, and some XRD peaks of metallic Ag appeared (Figure 1b), indicating $AgNO_3$ adsorbed onto the mesoporous silica materials has decomposed into Ag metal and gas phase at 300 °C in the experiment. The Ag peaks also suggest the existence of some large crystallites.

The N_2 adsorption−desorption isotherms of samples PS and AST can be classified as a type IV isotherm, typical of mesoporous solids. A sharp step occurs in each sample between $P/P_0 = 0.2$ and 0.3, which indicative of the filling of N_2 molecules in the mesopores. The sharpness of these steps reflects the uniform pore size. The isotherms contain an H3 hysteresis loop at high P/P_0 (0.4−1) as defined by IUPAC,[18] associated with solids with slit-shaped pores or platelike particles.

---

* Corresponding author.

(1) Braun, P. U.; Osenar, P.; Stupp, S. I. *Nature* **1996**, *380*, 325.

(2) Shenton, W.; Pum, D.; Sleytr, U. B.; Mann, S. *Nature* **1997**, *389*, 585.

(3) Chara, P. C.; Heath, J. R.; Gelbart, W. M. *Angew. Chem., Int. Ed. Engl.* **1997**, *36*, 1078.

(4) Braun, P. U.; Stupp, S. I. *Chem. Commun.* **1996**, 321.

(5) Motte, L.; Billoudet, F.; Lacaze, E.; Douin, J.; Pileni, M. P. *J. Phys. Chem. B* **1997**, *101*, 138.

(6) Korgel, B. A.; Fitzmaurice, D. *Adv. Mater.* **1998**, *10*, 661.

(7) Murray, C. B.; Kagan, C. R.; Bawendi, M. G. *Science* **1995**, *270*, 1335.

(8) Guo, S.; Popovitz-Biro, R.; Arad, T.; Hodes, G.; Leiserowitz, L.; Lahav, M. *Adv. Mater.* **1998**, *10*, 657.

(9) Korgel, B. A.; Fullam, S.; Connolly, S.; Fitzmaurice, D. *J. Phys. Chem. B* **1998**, *102*, 8379.

(10) Mirkin, C. A.; Letsinger, R. L.; Mucic, R. C.; Storhoff, J. J. *Nature* **1996**, *382*, 607.

(11) Harfenist, S. A.; Wang, Z. L.; Alvanrez, M. M.; Vezmar, I.; Whetten, R. L. *J. Phys. Chem.* **1996**, *100*, 13904.

(12) Kresge, C. T.; Leonowicz, M. E.; Roth, W. J.; Vartuli, J. C.; Beck, J. L. *Nature* **1992**, *359*, 710.

(13) Huo, Q.; Margolese, D. I.; Ciesla, U.; Demuth, D. G.; Feng, P.; Cier, T. E.; Sierger, P.; Firouzi, A.; Chmelka, B. F.; Schuth, F.; Stucky, G. D. *Chem. Mater.* **1994**, *6*, 1176.

(14) Raman, N. K.; Anderson, M. T.; Brinker, C. J. *Chem. Mater.* **1996**, *8*, 1682.

(15) Ciesla, U.; Schuth, F. *Microporous Mesoporous Mater.* **1999**, *27*, 131.

(16) Wu, C. G.; Bein, T. *Science* **1994**, *264*, 1757.

(17) Moller, K.; Bein, T. *Chem. Mater.* **1998**, *10*, 2950.

(18) Sing, K. S. W.; Everett, D. H.; Haul, R. A. W.; Moscou, L.; Pierotti, R. A.; Rouquerol, J.; Siemieniew, T. *Pure Appl. Chem.* **1985**, *57*, 603.

10.1021/cm990228p CCC: $18.00

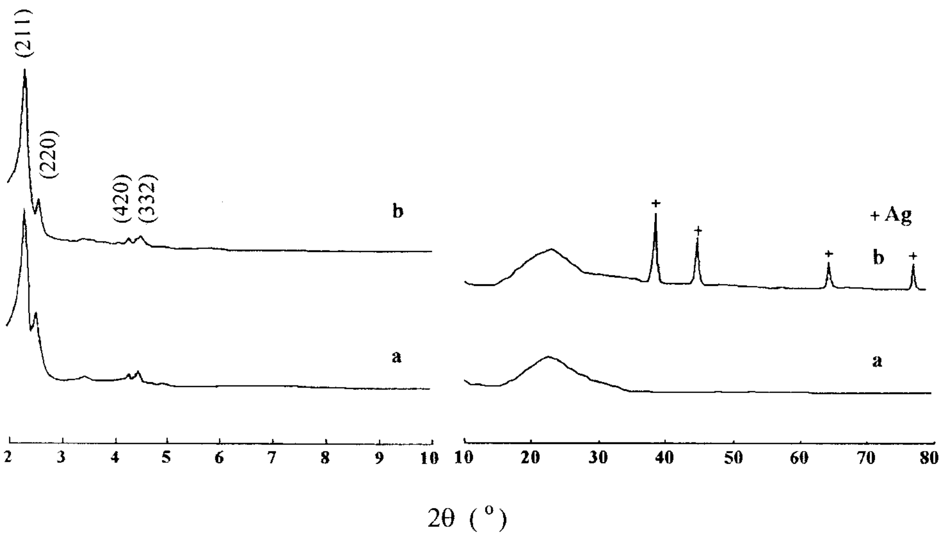

Figure 1. X-ray powder diffraction patterns of samples: (a) sample AS and (b) sample AST.

Table 1. Pore Structure Parameters of Mesoporous Silica Samples

sample	specific surface area S_{BET} (m^2/g)	pore volume V_{BJH} (cm^3/g)	average pore size D_{BJH} (Å)
PS	1152	1.013	26.44
AST	793	0.646	24.51

However, the amount of adsorbed N_2 of sample AST decreased compared to that of PS, and the pore structure parameters of samples listed in Table 1 show that specfic surface area (S_{BET}), total pore volume (V_{BJH}), and average pore size (D_{BJH}) values of Ag-loaded sample AST become smaller, which can be due to the loading of Ag metal onto the mesoporous silica materials.

Compared with the HREM image of sample PS (Figure 2a), some dark areas in the ordered pore structures of sample AST can clearly be seen (Figure 3a), which can be due to the surface deposits of Ag. Most interestingly, a large part of the Ag nanocrystalline deposits on the surface of mesoporous silica materials have regular and oriented arrangement and have a width of about 4 nm and are separated by a gap of about 1.8 nm. Compared with the diffraction pattern of pure MCM-48 material (Figure 2b), the SAD pattern of sample AST (Figure 3b) shows that two close diffraction spots appeared on both sides of transmission pattern. The fact that the two additional spots which appears as a line indicates the existence of one-dimensionally ordered Ag nanoarrays. The line-to-line distance of Ag nanoarrays, calculated on the basis of the formula of $d = L\lambda/R$, was about 5.6−5.8 nm, which is considerably larger than the lattice distance of mesopores. However, in the sample AS without thermal treatment, only a few nanoparticles adhered to the surface of mesoporous silica, which may be a complex compound of silver ions combined with nitrate, as can be seen in the TEM observation (not shown). Additionally, when the sample AST experienced a thermal treatment at 500 °C, the Ag nanoarrays can no longer be observed, leaving just some larger particles. Therefore, the Ag nanocrystal arrays may be formed through the reorganization of Ag superfine particles at a suitable temperature range.

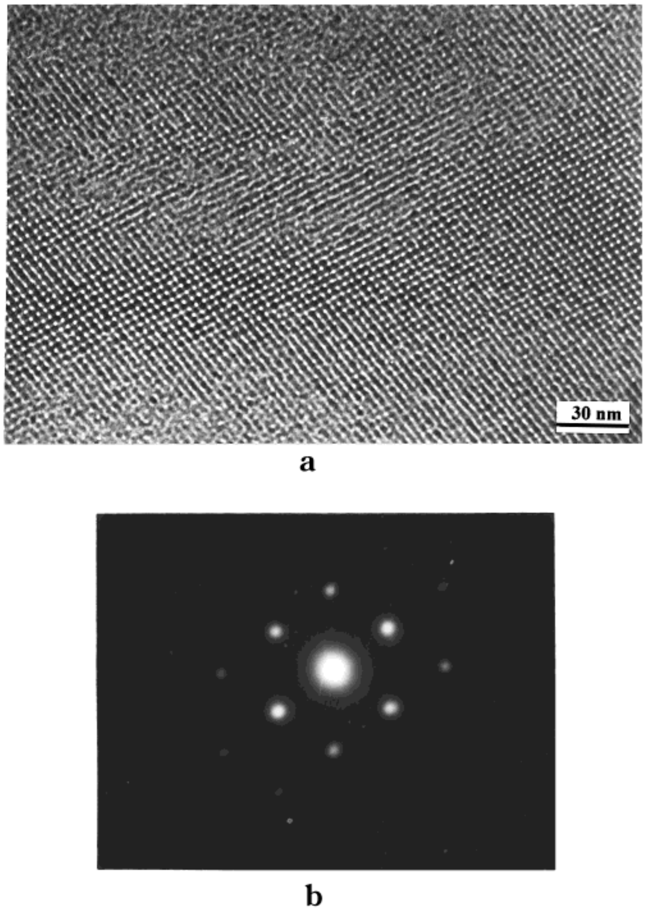

a

b

Figure 2. HREM image of sample PS (a) and its selected area electron diffraction pattern (b) along the [110] direction.

When $AgNO_3$ solution was dropped onto the mesoporous silica material, the nanopores could be filled with an $AgNO_3$−ethanol solution driven by capillary action, and the sample was thus soaked. Therefore, the mesochannels of material played a role of tiny tubes, each containing a small amount of $AgNO_3$ solution. When the solvent ethanol was evaporated, Ag^+ and NO_3^- ions could be adsorbed onto the surface of silica framework, since the nanometer-sized framework of silica has many dangling bonds and surface hydroxyl groups.[17] Therefore, a complex compound between Ag^+ and NO_3^-, which was identified by XRD to be a noncrystal structure, could be formed by adhering to the inner and outer

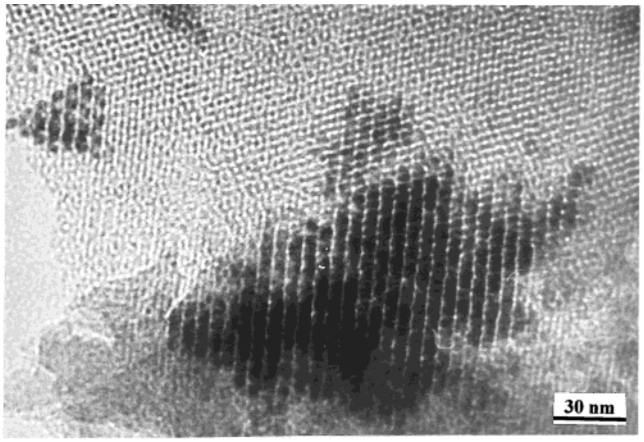

a

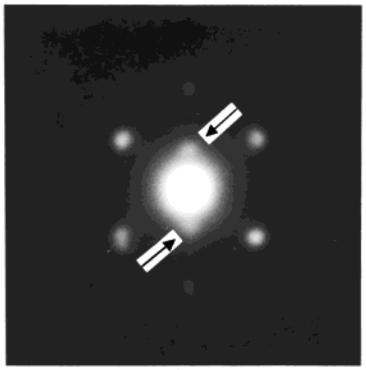

b

Figure 3. HREM image of Ag-loaded sample AST (a) and its selected area electron diffraction pattern (b) along the [110] direction.

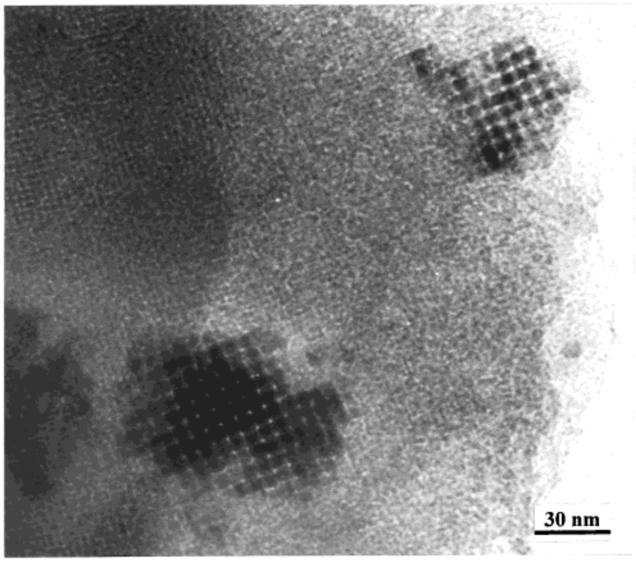

Figure 4. HREM image of sample AST loaded with square arrangement of Ag nanoarrays, in which the pore structures of the mesoporous silica substrate have been partly damaged by the electron beam.

surface of the material. With increasing thermal treatment temperature, decomposition occurred and the ultrafine Ag clusters were formed. It is well-known that huge excess free energy exists in nanoparticles, as a result, small metal clusters might be very mobile and are particularly easy to aggregate.[19,20] The Ag nuclei adsorbed on the inner or outer surface of the silica framework can be activated to overcome the kinetic energy barrier at a suitable temperature and to have energy to diffuse to the outer surface. The metallic bonds among metal clusters play an important role during the processes of diffusion and aggregation; however, the stress field of the substrate, such as line tension, elastic relaxation force and so on, could not be neglected.[21−23] Therefore, the self-aggregation process of Ag nuclei was inevitably influenced by the mesoscale stress field of periodic mesoporous structures. The regular mesochannels provide a lattice of uniform voids, where the stress fields are very different from the framework. To match with the periodical stress field of mesoporous silica substrates, some Ag nuclei could be reorganized on the periodically ordered cubic mesoporous silica surface. Moreover, the self-assembly of Ag could arrange into regular square, hexagonal, or other patterns. Figure 4 gives a picture of nanocrystalline Ag arranged in square-shaped networks, where the TEM observation using 200 keV at room temperature did not result in structural damage of Ag nanoarrays even the mesoporous frameworks has been partially destroyed, illustrating these Ag nanostructures have higher stability. When the sample AST received a thermal treatment at 500 °C, the high mobility and strong bonding force among Ag clusters became dominate and only larger Ag particles were obtained.

In summary, regular Ag nanocrystal line arrays loaded on the surface of mesoporous silica were observed for the first time. The influence of periodic surface stress field of the ordered mesopore structures on the arrangement of Ag clusters was argued to explain this novel phenomenon. This attempt may provide a new idea for the self-assembly of nanostructures on solid surfaces. However, further investigation is still needed to identify the intrinsic force that directs the nanocrystalline array formation.

Acknowledgment. This work was supported by the National Natural Science Foundation of China with contract no. 59882007.

CM990228P

---

(19) Conners, L.; Hollis, T.; Johnson, D. A.; Blyholder, G. *J. Phys. Chem. B* **1998**, *102*, 10112.

(20) Ying, J. Y.; Wang, G. H.; Fuchs, H.; Laschinski, R.; Gleiter, H. *Mater. Lett.* **1992**, *15*, 180.

(21) Seul, M.; Andelman, D. *Science* **1995**, *267*, 476.

(22) Zhang, Z. Y.; Lagally, M. G. *Science* **1997**, *276*, 377.

(23) Pohl, K.; Bartelt, M. C.; Figuera, J. D. I.; Bartelt, N. C.; Hrbek, J.; Hwang, R. Q. *Nature* **1999**, *397*, 238.